Aquatic Life and Ecosystems
https://www.sciltp.com/journals/ale

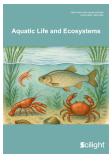

Article

Transcriptomic Analysis of Liver Response in Juvenile Yellowfin Tuna (*Thunnus albacares*) Under Acute Heat Stress

Junhua Huang [1,2,3,4,5], Zhengyi Fu [1,2,3,4,6], Jing Bai [7] and Zhenhua Ma [1,2,3,4,6,*]

[1] Key Laboratory of Efficient Utilization and Processing of Marine Fishery Resources of Hainan Province, Sanya Tropical Fisheries Research Institute, Sanya 572018, China
[2] South China Sea Fisheries Research Institute, Chinese Academy of Fishery Sciences, Guangzhou 510300, China
[3] Hainan Engineering Research Center for Deep-Sea Aquaculture and Processing, Sanya Tropical Fisheries Research Institute, Sanya 572018, China
[4] International Joint Research Center for Conservation and Application of Fishery Resources in the South China Sea, Sanya Tropical Fisheries Research Institute, Sanya 572018, China
[5] College of Fisheries and Life Sciences, Dalian Ocean University, Dalian 116023, China
[6] College of Science and Engineering, Flinders University, Adelaide, SA 5001, Australia
[7] Hainan Shuancheng Marine Technology Development Co., Ltd., Haikou 570100, China
* Correspondence: zhenhua.ma@scsfri.ac.cn

How To Cite: Huang, J.; Fu, Z.; Bai, J.; et al. Transcriptomic Analysis of Liver Response in Juvenile Yellowfin Tuna (*Thunnus albacares*) Under Acute Heat Stress. *Aquatic Life and Ecosystems* **2026**, *2*(1), 2. https://doi.org/10.53941/ale.2026.100002

Received: 22 September 2025
Revised: 5 December 2025
Accepted: 16 December 2025
Published: 7 January 2026

Abstract: Ocean warming driven by climate change has led to an increased frequency of extreme high-temperature events, posing serious threats to marine organisms. Yellowfin tuna (*Thunnus albacares*), a pelagic species with partial endothermic traits, holds high ecological and economic value but remains highly sensitive to acute thermal stress. In this study, we simulated heatwave conditions in the South China Sea by exposing juvenile yellowfin tuna to 34 °C (high-temperature group, HT) and 28 °C (control group, LT), and analyzed hepatic transcriptomic responses at 6 h and 24 h. A total of 778 and 524 differentially expressed genes (DEGs) were identified at 6 h and 24 h, respectively, with 155 shared DEGs. KEGG enrichment analysis showed that these common DEGs were significantly associated with key pathways such as protein processing in the endoplasmic reticulum, herpes simplex virus 1 infection, and antigen processing and presentation. Clustering analysis revealed that classical stress-response genes, including *hspa5*, *dnajc3a*, *hspa4l*, and *hsp90b1*, were significantly upregulated under heat stress. Protein–protein interaction (PPI) analysis further confirmed these genes as central hubs within molecular chaperone and protein-folding modules. In contrast, immune-related genes such as *MHC1*, *IFIH1*, and *KRAB* were downregulated and showed weak or no interactions in the network. This study provides molecular insights into the thermal stress response of yellowfin tuna and offers a theoretical basis for the development of heat-resilient breeding strategies and improved aquaculture management.

Keywords: heat stress; transcriptome; *Thunnus albacares*; KEGG enrichment; protein-protein interaction analysis

1. Introduction

In recent years, climate change has led to a global rise in ocean temperatures, with extreme thermal events such as marine heatwaves occurring with increasing frequency and intensity, posing a severe threat to marine ecosystems [1]. El Nino events are often accompanied by elevated sea surface temperatures (SSTs) in the central and eastern equatorial Pacific, triggering widespread climate anomalies, particularly in Asia where SSTs tend to

rise significantly [2,3]. These abnormal warming events not only disrupt ecological stability in the South China Sea but also exert profound effects on aquatic organisms in the region [4]. Water temperatures, as a critical environmental factor, directly influences the physiological metabolism and adaptive strategies of aquatic organisms [5]. For fish, elevated temperatures represent a potent environmental stressor, often resulting in increased oxygen demand, growth inhibition, and reproductive dysfunction [6,7]. Studies have shown that rapid increases in temperature can trigger secondary stress responses in fish, including elevated glucose and lactate levels, along with osmotic imbalances during heat stress [8]. Moreover, Munday et al. reported that *Acanthochromis polyacanthus* exhibited reduced growth rates under thermal stress at 31 °C [9]. Collectively, these findings suggest that high-temperature stress can severely disrupt energy metabolism and osmoregulation in fish, impairing growth and development and ultimately threatening fish health and population stability.

Yellowfin tuna (*Thunnus albacares*), a widely distributed pelagic species inhabiting tropical and subtropical oceans, holds substantial economic and ecological value [10]. Although tunas are ectothermic fish, *T. albacares* possesses heat-conserving physiological features—often described as regional endothermy—that allow it to maintain elevated temperatures in specific tissues such as red muscle, the brain, and viscera [11]. This regional endothermy enables yellowfin tuna to tolerate and buffer moderate fluctuations in ambient temperature far more effectively than most teleost fishes, distinguishing it from typical ectothermic marine species [12]. However, it still experiences pronounced physiological stress under extreme thermal conditions [13]. Previous studies have revealed that elevated temperatures can induce significant alterations in the metabolic processes, immune regulation, and behavioral patterns of tunas [14,15]. For instance, Liu et al. reported that under acute thermal stress at 34 °C, the activities of superoxide dismutase (SOD) in the liver and gill tissues of yellowfin tuna increased significantly at both 6 h and 24 h, indicating the activation of an antioxidant response within a short timeframe [16]. Concurrently, energy reserves in the muscle tissue were markedly depleted [17]. These findings demonstrate that although *T. albacares* can moderate thermal variability, it still mounts strong and measurable physiological and molecular responses under thermal challenge. Together with its ecological relevance, broad distribution, and well-characterized thermal physiology, these characteristics support the use of yellowfin tuna as an informative and biologically meaningful model for investigating heat-stress mechanisms in pelagic marine fish.

The liver, as a principal immune and metabolic organ in fish, plays a central role in maintaining physiological homeostasis and orchestrating responses to environmental stressors [18]. Beyond its involvement in energy metabolism and nutrient storage, the liver also regulates antioxidant defense and immune responses [19,20]. Previous studies have demonstrated that high-temperature stress can induce pronounced physiological and molecular alterations in fish liver, including disruptions in lipid metabolism, elevated oxidative stress, and aberrant expression of immune-related genes. For example, exposure of *Sander lucioperca* to 34 °C heat stress has been reported to trigger a vicious cycle between hepatic H_2O_2 accumulation and pro-inflammatory cytokines, along with P53-mediated mitochondrial apoptosis [21]. Similarly, in *Labeo rohita*, rearing at extremely high temperatures of 37–38 °C for two weeks resulted in a 30% mortality rate, accompanied by marked pro-inflammatory responses and oxidative damage [22]. These findings underscore the liver's sensitivity to thermal stress and its pivotal role in systemic stress adaptation.

Heat stress induces a cascade of molecular responses involving oxidative stress, inflammatory cytokine release, apoptosis, and disturbances in energy metabolism [23]. However, most previous studies have focused on individual indicators or specific signaling pathways, limiting our understanding of the liver's global molecular regulatory landscape under thermal stress. With the advent of high-throughput sequencing technologies, transcriptomics has emerged as a powerful tool to systematically investigate organismal responses to environmental challenges [24]. Transcriptomic analyses have identified core gene networks involved in heat stress responses across various fish species, including *Clarias fuscus* [25], *Danio rerio* [26], *Salmo salar* [27], and *Scophthalmus maximus* [28], providing valuable genomic resources and theoretical foundations for elucidating molecular adaptation mechanisms in fish under thermal stress.

In the present study, we established a high-temperature stress condition of 34 °C, based on recorded sea surface temperatures during summer and marine heatwave events in the South China Sea in recent years, where temperatures have exceeded 34 °C [29,30]. This temperature closely approaches the upper thermal threshold that *Thunnus albacares* may encounter in its natural habitat. Nevertheless, comprehensive studies on the molecular and physiological responses of *T. albacares* liver under acute heat stress remain limited. Therefore, we simulated an acute thermal stress scenario representative of natural marine conditions and systematically evaluated the multidimensional physiological responses of juvenile *T. albacares* exposed to high temperature (34 °C) compared to optimal temperature (28 °C) at two time points (6 h and 24 h). Specifically, we integrated transcriptomic profiles obtained from RNA-Seq together with qPCR validation to elucidate the molecular responses of yellowfin tuna to thermal stress, focusing on pathways related to metabolic regulation, immune activation, and oxidative stress.

Through transcriptomic profiling, this study aims to elucidate the physiological and molecular strategies adopted by *T. albacares* to cope with acute thermal stress. The findings are expected to enhance our understanding of heat adaptation mechanisms in this species and provide a scientific foundation for sustainable resource management and health-oriented aquaculture under climate change scenarios.

2. Materials and Methods

2.1. Experimental Fish and Design

Juvenile *Thunnus albacares* were initially reared in offshore sea cages located in Xincun Harbor, Xincun Town, Lingshui County, Hainan Province, China. They were then transferred to the Sanya Tropical Fisheries Research Institute for a 7-day acclimation period. During this period, fish were maintained in an indoor recirculating aquaculture system under controlled rearing conditions. The water temperature was maintained at 28.0 ± 0.5 °C, which corresponded to the ambient water temperature at the time the experiment was conducted, rather than a direct representation of natural habitat conditions, dissolved oxygen above 5.27 mg/L, ammonia nitrogen below 0.1 mg/L, pH at 7.57 ± 0.12, and salinity at 32‰. Dissolved oxygen, ammonia nitrogen, and pH were measured using commercial rapid test kits (Hach, Loveland, CO, USA) following the manufacturer's protocols, while salinity was measured using a handheld refractometer (ATAGO, Tokyo, Japan). Fish were fed fresh chopped fish pieces (approximately 4 cm × 2 cm) at a daily feeding rate of 5–8% of body weight.

At the beginning of the experiment, 60 juvenile yellowfin tuna were randomly assigned to a control group (LT, 28 °C) and a heat stress group (HT, 34 °C), with three independent tanks per group. The fish had an average body length of 28.03 ± 1.78 cm and an average weight of 503.23 ± 36.78 g. Both groups were maintained in 3000 L tanks. The HT group was gradually heated from the baseline temperature of 28 °C to 34 °C at a rate of 2 °C per hour using immersion heaters (Zhejiang Sensen Group Co., Ltd., Zhoushan, China). The heating rate of 2 °C/h was chosen because it is widely used in acute heat stress studies on marine fishes and effectively induces thermal stress without causing immediate mortality [21]. At the beginning of the experiment, 60 juvenile yellowfin tuna were randomly assigned to a control group (LT, 28 °C) and a heat stress group (HT, 34 °C), with three independent tanks per group (10 fish per tank). After reaching the target temperature, tissue sampling was conducted at 6 h and 24 h. At each sampling time point, three fish were randomly selected from each tank and euthanized with an overdose of MS-222. Liver tissues from the three individuals within the same tank were pooled to generate one biological replicate, resulting in three biological replicates per group per time point (totaling 12 RNA-Seq libraries). All collected samples were immediately frozen in liquid nitrogen and stored at −80 °C for subsequent analyses.

2.2. Transcriptome Library Construction

Total RNA was isolated from liver tissues using TRIzol reagent (Invitrogen, Carlsbad, CA, USA) according to the manufacturer's instructions. RNA quality and quantity were evaluated by agarose gel electrophoresis, NanoDrop 2000 spectrophotometry (NanoDrop Technologies, Wilmington, DE, USA), and an Agilent 2100 Bioanalyzer. Only high-quality RNA samples meeting the following criteria were used for subsequent analyses: OD260/280 between 1.8 and 2.2, OD260/230 ≥ 2.0, RNA Integrity Number (RIN) ≥ 7.0, and total RNA > 10 μg.

Transcriptome libraries were prepared using the TruSeq™ RNA Sample Preparation Kit (Illumina, San Diego, CA, USA) from 5 μg of total RNA, polyadenylated mRNA was enriched using oligo(dT) magnetic beads, followed by fragmentation and first- and second-strand cDNA synthesis using random hexamer primers (Illumina). The resulting cDNA underwent end repair, phosphorylation, and addition of an 'A' base according to the Illumina library preparation protocol. After quantification using the TBS380 fluorometer, paired-end RNA-seq libraries were sequenced on the Illumina HiSeq X Ten platform (2 × 150 bp reads) [31]. Each library generated approximately 45–50 million clean paired-end reads per sample (range: 42.1–57.8 million), providing sufficient depth for transcriptome profiling and downstream analyses.

2.3. Sequencing Data Quality Control and Assembly

To ensure the accuracy of transcriptomic analysis, raw sequencing reads underwent stringent quality filtering using Trimmomatic v0.39 [32]. Adapter sequences were trimmed, and reads containing >10% unidentified nucleotides (N) or >50% bases with Qphred ≤ 10 were discarded. After quality control, high-quality clean reads were retained for subsequent analyses.

2.4. Genome-Guided Alignment and Transcript Assembly

Clean reads were aligned to the *Thunnus albacares* reference genome using HISAT2 v2.2.1 with default parameters [33]. Alignment files were then assembled into transcripts using StringTie v2.1.7 [34], enabling genome-guided transcript reconstruction and accurate estimation of gene and transcript abundances. Gene-level count matrices generated by StringTie were subsequently used for differential expression analysis.

2.5. Differential Expression and KEGG Pathway Enrichment Analysis

Gene-level raw counts from StringTie were imported into DESeq2 v1.36.0 for differential expression analysis [35]. Only raw counts (not TPM values) were used for normalization and statistical testing. Genes with an adjusted *p*-value < 0.05 (Benjamini–Hochberg correction) and $|\log_2(\text{fold change})| > 2$ were considered significantly differentially expressed. To examine gene expression patterns, TPM values generated by StringTie were used only for visualization and low-expression filtering, and not for DESeq2 [36].

To further explore the biological roles of DEGs, KEGG enrichment analysis was conducted using the KOBAS platform (http://kobas.cbi.pku.edu.cn/home.do, accessed on 11 Aug 2025). Enrichment tests used all annotated protein-coding genes in the *T. albacares* reference genome as the background gene set. Pathways with a Bonferroni-adjusted *p*-value < 0.05 were considered significantly enriched. Hierarchical clustering was performed in R using the hclust function, and gene–gene correlations were evaluated using Spearman coefficients to construct co-expression networks [37].

2.6. Protein-Protein Interaction (PPI) Analysis

The PPI network was constructed using STRING v11.5 (https://www.stringdb.org , accessed on 11 August 2025) [38]. with *Danio rerio* selected as the reference species due to its high-quality genome annotation and phylogenetic proximity to *Thunnus albacares*. Only high-confidence interaction pairs (combined score ≥ 0.70) based on experimental data, curated databases, and co-expression evidence were retained. The resulting interaction file was imported into Cytoscape v3.9.1, where network topology parameters—including node degree, edge number, and connectivity—were calculated using the NetworkAnalyzer plugin. Genes with high node degrees were identified as hub genes. The final PPI network was visualized using Cytoscape.

2.7. Validation of RNA-Seq Results by Quantitative Real-Time PCR (qRT-PCR)

Eight immune-related genes were subjected to quantitative real-time PCR (qRT-PCR) to validate the RNA-Seq results, using a real-time PCR system (Analytik Jena GmbH, Jena, Germany) and SYBR Green mix (Tiangen Biotech Co., Ltd., Beijing, China). These genes were selected because they represent key immune- and stress-related functional categories and cover a range of high, medium, and low expression levels in the RNA-Seq dataset, allowing assessment of expression trend consistency rather than differential-expression significance. Gene-specific primers were designed based on transcriptome data using Primer Premier 5.0 (Table 1) [39]. Each 20 μL reaction mixture contained 10 μL of 2× RealUniversal PreMix, 0.6 μL of each primer (10 μM), and 2 μL of diluted cDNA. The qPCR conditions were as follows: initial denaturation at 95 °C for 15 min, followed by 40 amplification cycles (95 °C for 10 s, 58 °C for 20 s, and 72 °C for 30 s). A melting curve analysis was performed at the end of each amplification to ensure specific amplification and the absence of primer-dimer formation. No-template controls were included in all assays to confirm the absence of contamination in the PCR reactions.

The relative mRNA expression levels of target genes were calculated using the $2^{-\Delta\Delta Ct}$ method, normalized to the expression of the *β-actin* gene as the internal reference. The stability of *β-actin* under heat-stress conditions was confirmed prior to its use, as it showed no significant variation in RNA-Seq data and exhibited consistent Ct values across all samples. Gene expression in the CG group at 0 h was used as the baseline. Amplification efficiencies ranged from 90% to 110%. The qRT-PCR results were used to evaluate the consistency of expression trends (direction of change) with RNA-Seq rather than to validate the exact fold-change magnitude or DEG significance thresholds. The expression profiles of the chosen genes from qRT-PCR were assessed against RNA-Seq data for consistency.

Table 1. qRT-PCR primers for immune-related genes in *Thunnus albacares*.

Gene Abbreviation	Primer Sequence (5′–3′)	Amplicon Size (bp)
β-actin	F: TCCCTGTATGCCTCTGGT	217
	R: TGATGTCACGCACGATTT	
hspa8b	F: GTTATGTTGCCTTCACCG R: GTACTCCACCTTTACTTTCG	203
cat	F: TGACAGGCAACAACACCC R: ATCGCTAAACAGGAAGGACA	173
gpx1b	F: GGCACAATAATGGCTAAA	143
	R: GTGTAATCCCTGGTGGTC	
sod1	F: GCAGCGATAACTCAGTCT R: TATGCTAAGCCAACCTAC	127
irf3	F: AGCCAAACTGACCCAACG R: GGTTCTTGGCAGCATCTC	215
acadm	F: AGAAGAGTTGGCTTATGG	184
	R: TGAGAAGTGGTGGTAGGA	
lpl	F: AAGAATCGGCTTAGTTTAG R: TTATGAATCCTCCCTGCT	218
b2m	F: GCAACAGTAGGCAGTCAG R: TCCTTCTTTACCCACATT	179

2.8. Statistical Analysis

All RNA-Seq differential expression analyses were performed using DESeq2, with adjusted $p < 0.05$ considered statistically significant. The design formula used in DESeq2 was design = Group + Time to account for differences between experimental treatments. All bar charts were generated using Origin 2022 software.

3. Results

3.1. Transcriptome Sequencing, Assembly, and Analysis of DEG Changes over Time under Different Heat Stress Conditions

The average sequencing and assembly metrics of transcriptome data across different time points and treatment groups are summarized in Table 2. After quality filtering, a total of 560,563,082 high-quality clean reads were obtained. On average, each sample generated approximately 45–50 million clean reads, which is sufficient for transcriptome-wide analysis following rRNA removal during library preparation. Over 92.43% of reads had a Q-score ≥ Q30, and the mean GC content was 50.93%. Principal component analysis (PCA, Figure 1) revealed that PC1 and PC2 accounted for 31.63% and 12.92% of the total variance, respectively. Although some overlap was observed among samples, biological replicates generally exhibited similar expression patterns within each treatment group. Notably, the HT6h, HT24h, LT6h, and LT24h samples were partially separated along both PC1 and PC2 axes, suggesting distinct transcriptomic shifts among treatments despite within-group variability.

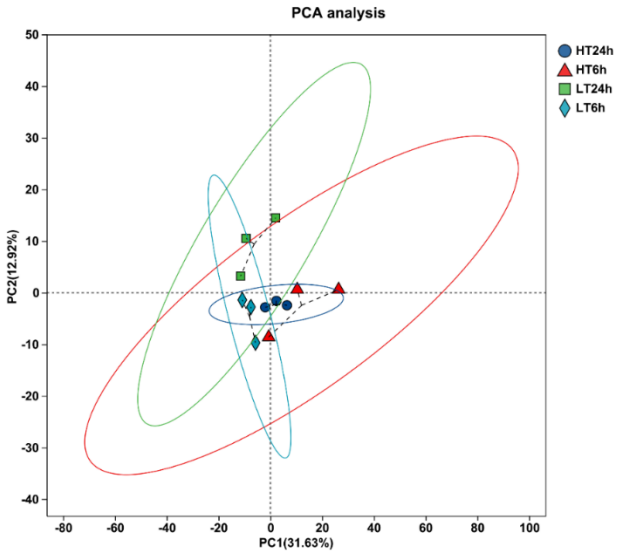

Figure 1. Principal component analysis (PCA) of samples from different groups. The circles indicate the 95% confidence intervals for samples belonging to the same group (groups are distinguished by color).

According to the volcano plot analysis of DEGs between the HT and LT groups at 6 h (Figure 2A), a total of 778 significant DEGs were identified, including 482 upregulated and 296 downregulated genes ($p < 0.05$). At the 24 h time point (Figure 2B), 524 DEGs were detected, comprising 244 upregulated and 280 downregulated genes ($p < 0.05$). Venn diagram analysis (Figure 2C) revealed that 155 DEGs were shared between the twotime points, while 623 DEGs were specific to 6 h and 369 DEGs to 24 h.

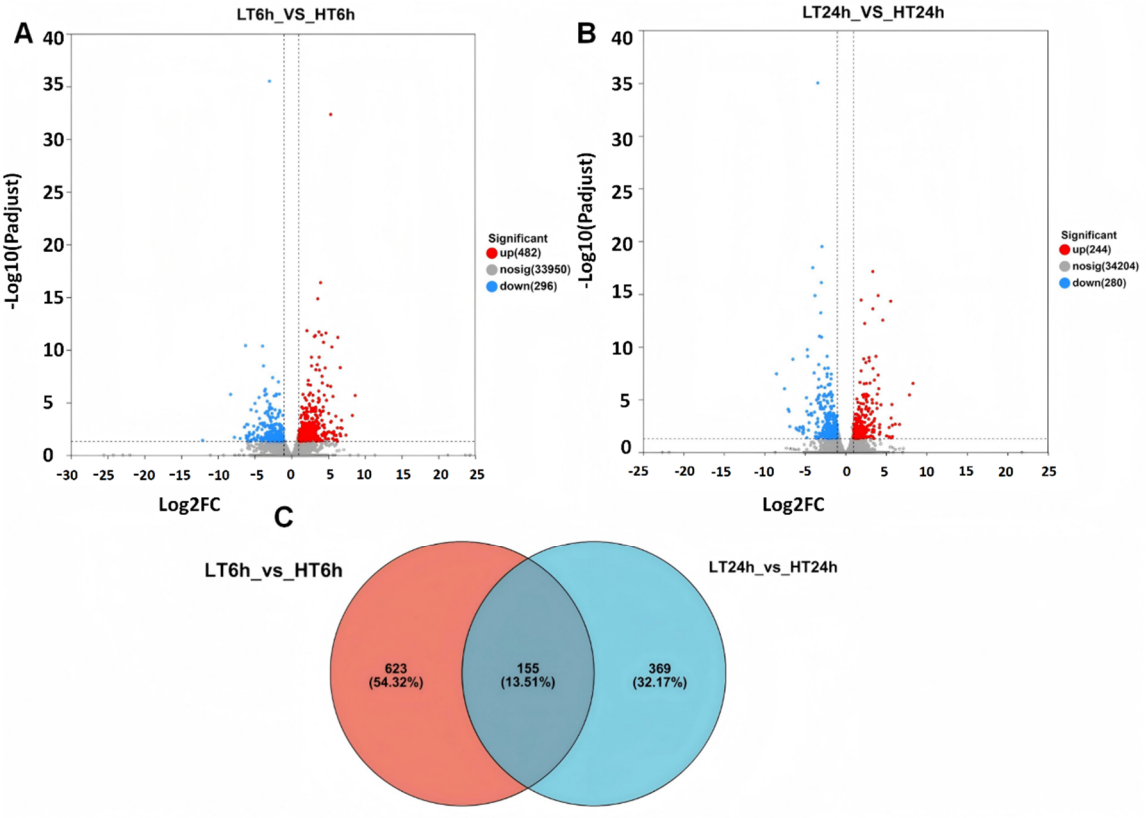

Figure 2. DEGs between the HT and LT groups at 6 h and 24 h. (**A**) Volcano plot of DEGs in the HT6h vs. LT6h comparison. Red and blue dots represent significantly upregulated and downregulated genes, respectively ($p < 0.05$; $|\log_2 FC| > 1$); (**B**) Volcano plot of DEGs in the HT24h vs. LT24h comparison. Red and blue dots indicate significantly upregulated and downregulated genes, respectively ($p < 0.05$; $|\log_2 FC| > 1$); (**C**) Venn diagram showing the overlap of DEGs between the HT and LT groups at 6 h and 24 h.

To validate the RNA-Seq expression profiles, eight genes were examined using qRT-PCR. The relative expression patterns determined by qRT-PCR were consistent with those obtained from the RNA-Seq analysis, confirming the reliability of the transcriptomic data (Figure S1).

Table 2. Summary of RNA-seq data quality for LT and HT groups at 6 and 24 h.

Sample	Raw Reads	Clean Reads	GC Content (%)	Q30 (%)
LT6h-1	56391210	53804672	50.92	92.9
LT6h-2	49039678	47031648	50.85	92.45
LT6h-3	47327214	45227900	51.08	93.22
HT6h-1	48080862	45910332	50.97	92.77
HT6h-2	47853256	45884070	51.15	92.43
HT6h-3	43624808	42075020	50.22	92.87
LT24h-1	46655976	44727834	50.95	93.08
LT24h-2	46794620	44971918	50.95	92.36
LT24h-3	46759816	44419906	51.17	92.62
HT24h-1	46639070	44796650	51.08	92.69
HT24h-2	45946898	43937726	50.98	93.1
HT24h-3	60883394	57775406	50.8	92.84

3.2. KEGG Annotation and Enrichment Analysis of Shared DEGs at Both Time Points

To further investigate the functional characteristics of the DEGs shared at both time points, KEGG functional annotation and enrichment analyses were performed. KEGG annotation revealed that the top 20 pathways were mainly classified into six functional categories, including Metabolism, Genetic Information Processing, Environmental Information Processing, Cellular Processes, Organismal Systems, and Human Diseases (Figure 3A). Among these, most genes were associated with signal transduction, followed by pathways related to protein folding and degradation, cell growth and death, material transport and catabolism, and immune system processes.

KEGG enrichment analysis (Figure 3B) identified three pathways that were significantly enriched ($p < 0.05$), namely Protein processing in endoplasmic reticulum, Herpes simplex virus 1 infection, and Antigen processing and presentation. According to the enrichment results (Table S1), Protein processing in endoplasmic reticulum was categorized under Genetic Information Processing, with the secondary category of Folding, sorting and degradation. Herpes simplex virus 1 infection belonged to Human Diseases, with the secondary category of Infectious diseases: viral. Antigen processing and presentation was classified under Organismal Systems, with the secondary category of Immune system.

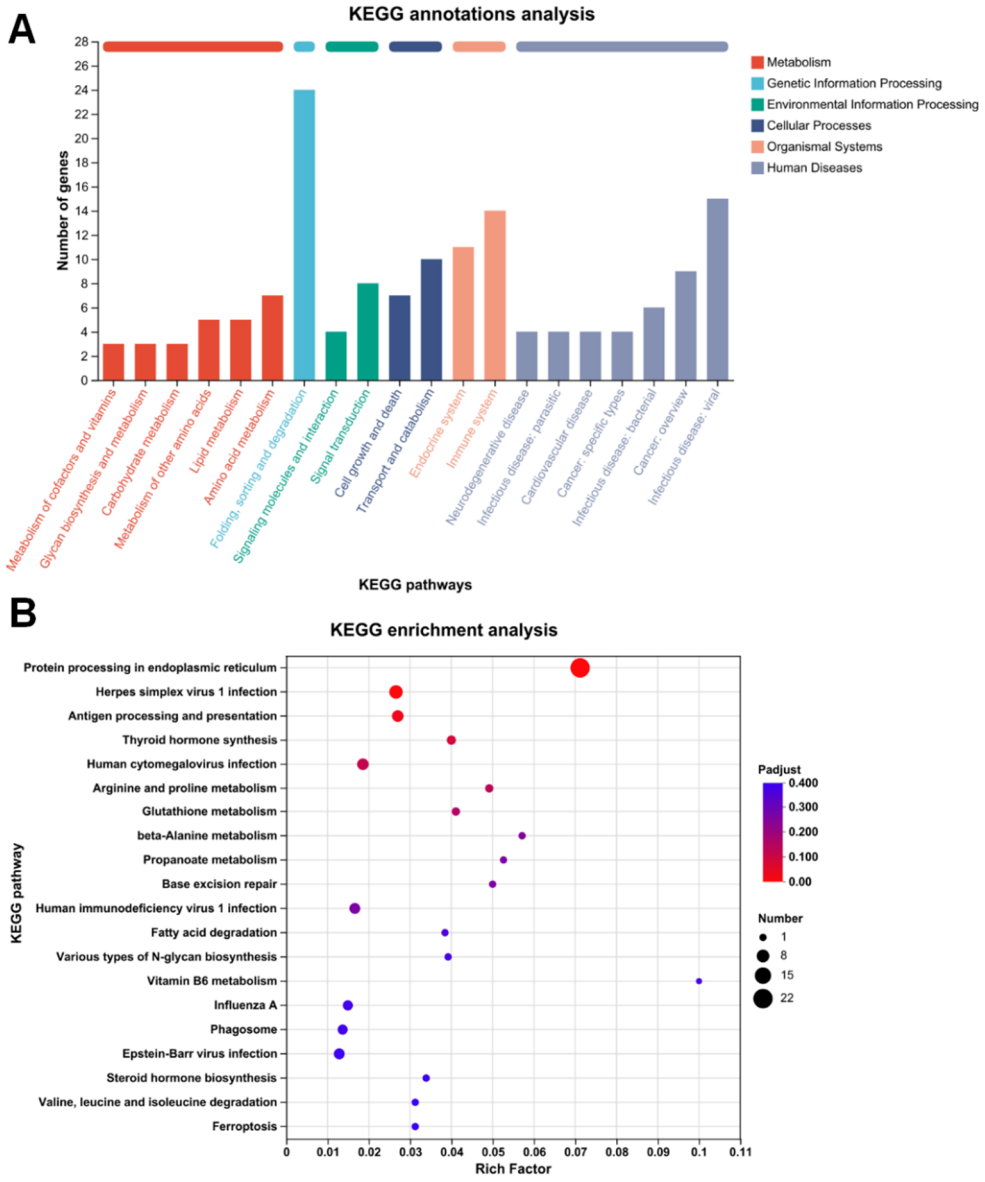

Figure 3. KEGG functional annotation and enrichment analysis of common DEGs at 6 h and 24 h in the LT and HT groups. (**A**) Annotation results of the top 20 KEGG pathways; (**B**) KEGG enrichment analysis of the common DEGs. The bubble plot shows significantly enriched pathways ($p < 0.05$). The x-axis represents the enrichment factor (Rich factor), bubble size indicates the number of genes, and bubble color corresponds to the adjusted p-value (Padjust).

3.3. KEGG Enrichment Analysis of Heat Stress-Specific DEGs at Each Time Point

To obtain a broader functional overview of temperature-induced transcriptomic responses, KEGG enrichment analyses were further conducted separately for DEGs uniquely induced by heat stress at 6 h and 24 h (Figure 4).

At 6 h, the unique DEGs in the comparison between the LT and HT groups were significantly enriched in 5 KEGG pathways ($p < 0.05$), including "Protein processing in endoplasmic reticulum", "Ascorbate and aldarate metabolism", "Protein export", "Porphyrin and chlorophyll metabolism", and "Drug metabolism—other enzymes" (Figure 4A; Table S2). In contrast, at 24 h, the unique DEGs in the comparison between the T and HT groups were significantly enriched in 14 KEGG pathways ($p < 0.05$), including "Influenza A", "Epstein-Barr virus infection", "Coronavirus disease—COVID-19", "Herpes simplex virus 1 infection", "Malaria", "Glutathione metabolism", "NOD-like receptor signaling pathway", "Hepatitis B", "Arginine and proline metabolism", "RIG-I-like receptor signaling pathway", "Toll-like receptor signaling pathway", "Cytosolic DNA-sensing pathway", "Antigen processing and presentation", and "Kaposi sarcoma-associated herpesvirus infection" (Figure 4B; Table S3).

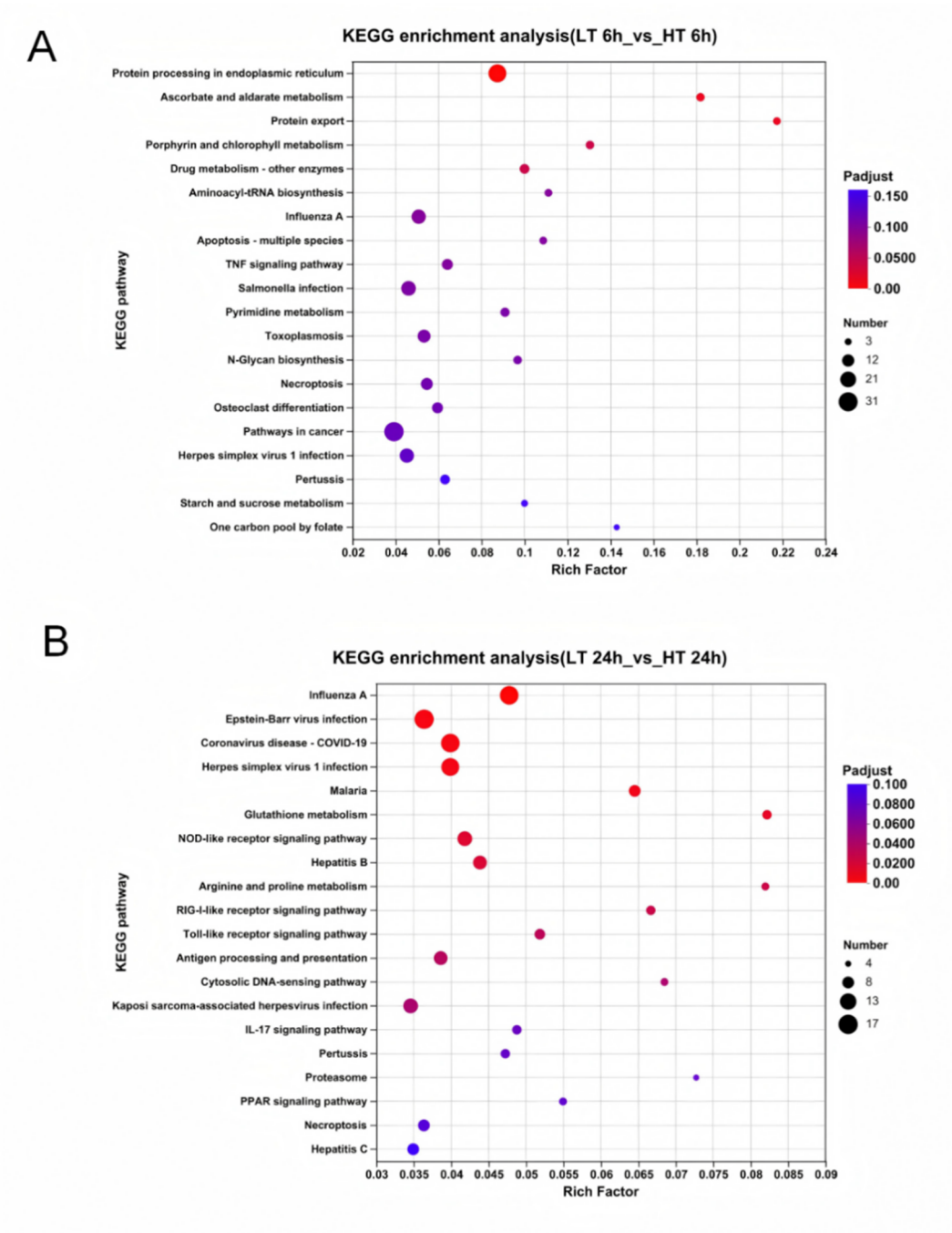

Figure 4. KEGG enrichment analysis of heat stress–specific DEGs at two sampling time points. (**A**) KEGG pathways significantly enriched by DEGs uniquely induced under heat stress at 6 h (HT 6 h vs. LT 6 h); (**B**) KEGG pathways significantly enriched by DEGs uniquely induced under heat stress at 24 h (HT 24 h vs. LT 24 h).

3.4. Cluster Heatmap Analysis

A cluster heatmap analysis was performed for 27 genes involved in significantly enriched KEGG pathways ($p < 0.05$) shared by DEGs between the LT and HT groups at both 6 h and 24 h (Figure 5). Two distinct expression patterns were observed. Specifically, the genes *hspa4l*, *os9*, *rheb*, *uggt1*, *sel1l*, *dnajc3a*, *sil1*, *syvn1*, *calr3a, hyou1*, *SEC24*, *pdia4*, *hapa5*, *dnajb11*, *pdia3*, *CALR*, *lman2*, *pdia6*, *hsp90b1*, *lman1*, *calr*, *herpud1*, and *GRP58* were significantly upregulated in the HT group at both time points compared to the LT group ($p < 0.05$). In contrast, *KRAB*, *ifih1*, *MHC1*, and *srsf5b* were significantly downregulated under the same conditions ($p < 0.05$).

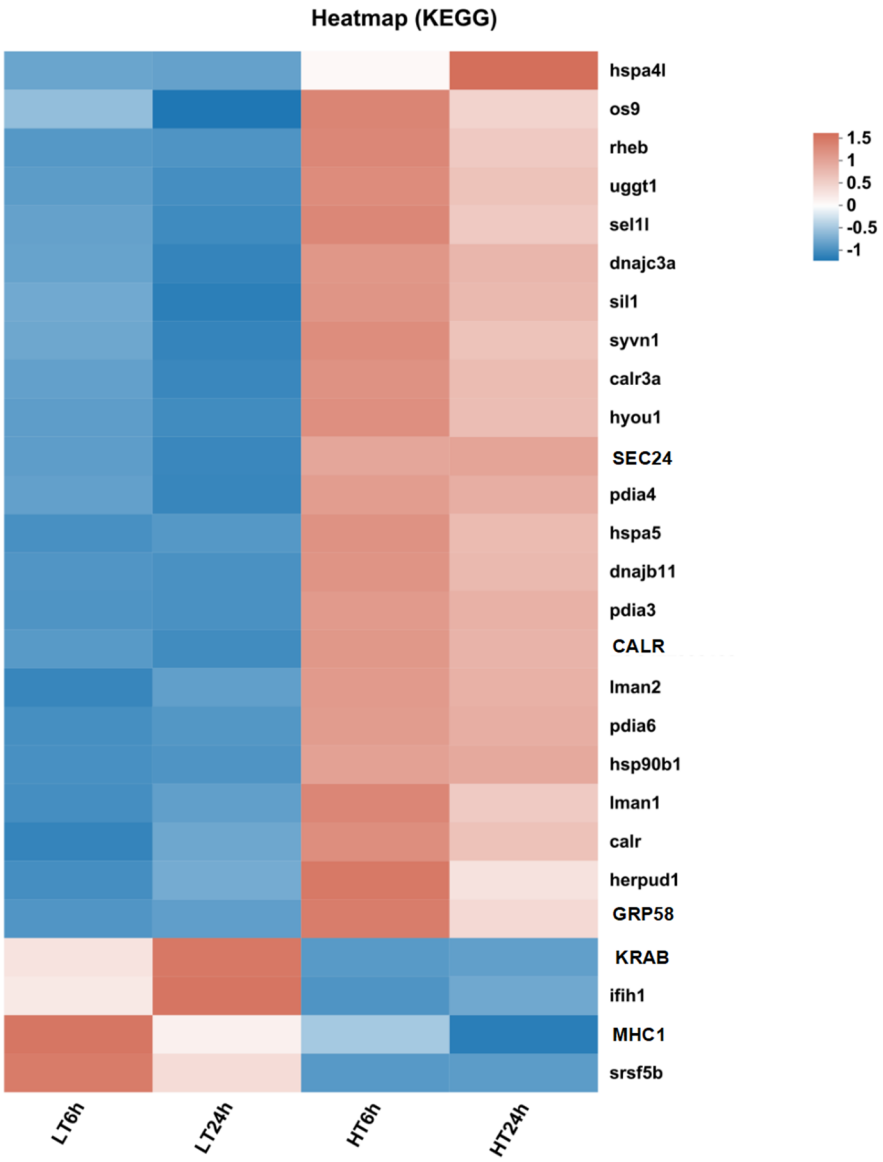

Figure 5. Heatmap showing normalized expression patterns (TPM, Z-score transformed) of representative genes enriched in KEGG pathways among DEGs detected at 6 h and 24 h in LT and HT groups. The heatmap represents standardized expression trends rather than pairwise log fold-change values. Genes were selected from significantly enriched KEGG pathways shared at both sampling time points to illustrate core transcriptional responses under heat stress.

3.5. PPI Network Analysis

Based on the significantly enriched KEGG pathways of the shared DEGs between the LT and HT groups at 6 h and 24 h, a PPI network was constructed (Figure 6). A total of 27 genes were incorporated into the analysis, forming a compact interaction network with high overall connectivity. Most of the genes were interconnected through multiple edges, indicating extensive interaction relationships.

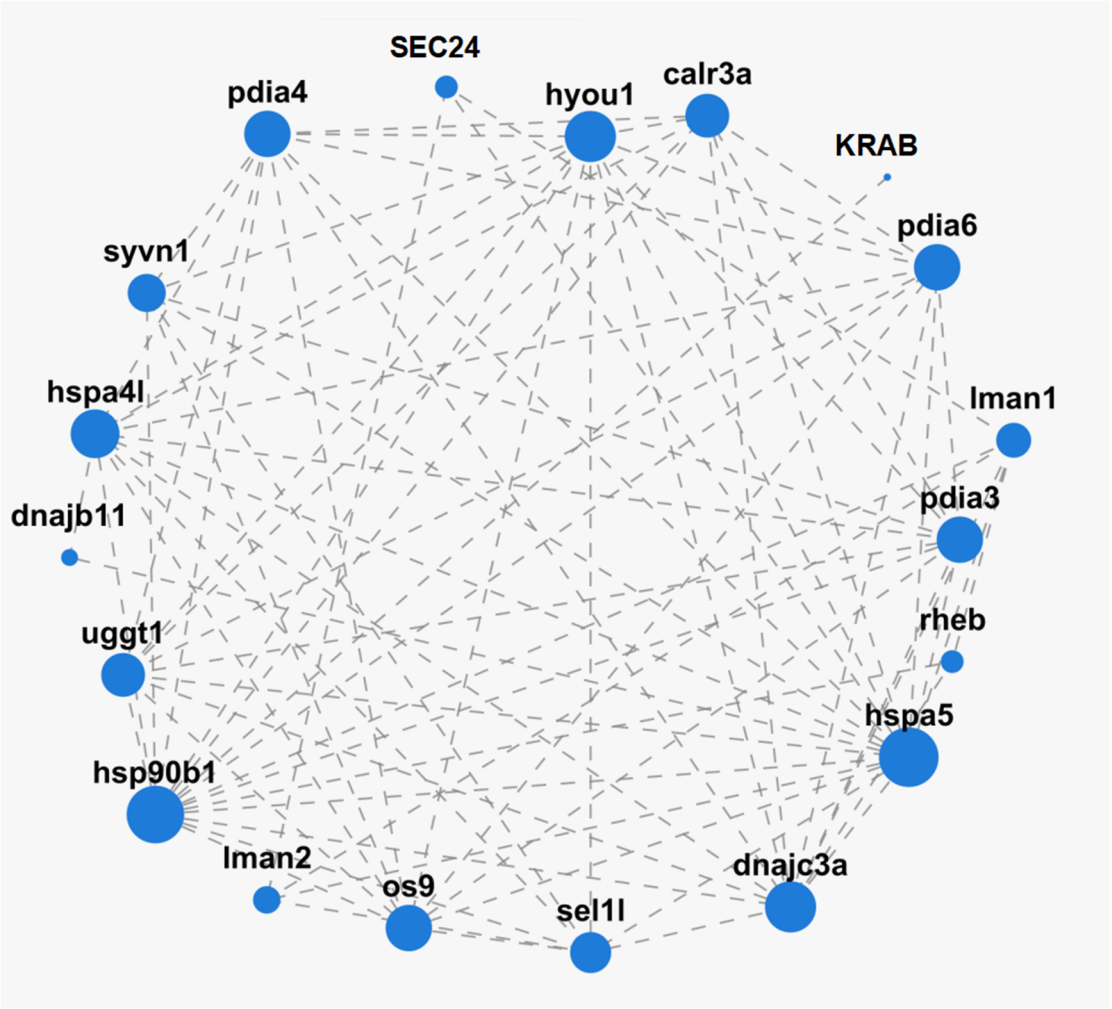

Figure 6. Protein–protein interaction (PPI) network of genes involved in significantly enriched KEGG pathways of shared DEGs between the LT and HT groups at 6 h and 24 h. Node size represents the degree of interaction.

Within the network, several genes exhibited high node degrees and occupied central hub positions, including *pdia4*, *hyou1*, *calr3a*, *pdia6*, *hsp90b1*, *hspa5*, *dnajc3a*, and *hspa4l*. These genes showed the largest number of connections and formed the core of the network. In contrast, genes such as *KRAB*, *SEC24*, *rheb*, and *dnajb11* displayed lower connectivity and were located at the periphery of the network.

The network could be roughly divided into two major interaction modules. The first module was dominated by *pdia4*, *pdia3*, *pdia6, hsp90b1*, *CALR*and *GRP58*, mainly consisting of genes associated with protein folding and endoplasmic reticulum protein processing, which were densely interconnected. The second module centered on *hspa4l*, *hspa5*, *hyou1*, *syvn1*, *uggt1*, and *dnajc3a*, which were primarily involved in molecular chaperones and signal regulation. In contrast, genes such as *KRAB*, *SEC24*, and *rheb* exhibited smaller node sizes and lower degrees of connectivity, and were located at the peripheral regions of the network. Although *MHC1*, *srsf5b*, and *ifih1* were significantly downregulated at the transcriptomic level, they did not form prominent interaction nodes within the PPI network.

4. Discussion

In this study, we also selected the liver as the target tissue, as it plays a pivotal role in the physiological response of fish to heat stress. Previous studies have shown that under thermal stress, the liver contributes to cellular homeostasis by regulating the expression of heat shock proteins, modulating antioxidant enzyme activities, and activating endoplasmic reticulum (ER) stress pathways [39]. Under high-temperature treatment at 34 °C, we conducted differential transcriptomic analyses of yellowfin tuna subjected to 28 °C and 34 °C at two time points (6 h and 24 h). The results revealed that the number of DEGs unique to the early heat stress phase (6 h) reached 623, which was considerably higher than the 369 DEGs identified at 24 h. This suggests that acute thermal stress triggers a more intense and rapid molecular response in the early phase, involving stress perception, signal transduction, and the activation of acute protective mechanisms [40]. By 24 h, the expression of some genes had stabilized, indicating

that the organism may have initiated adaptive responses to mitigate the ongoing impact of heat stress. These findings highlight the temporal and dynamic regulation of hepatic responses to thermal challenge in fish [41].

Subsequent KEGG enrichment analysis further elucidated the key functional pathways associated with these DEGs. Notably, the DEGs common to both the 6 h and 24 h time points were mainly enriched in pathways such as "Protein processing in endoplasmic reticulum" and "Antigen processing and presentation." Although KEGG annotates one of the enriched pathways as "Herpes simplex virus 1 infection," this pathway is widely recognized to contain conserved components related to ER stress, antigen presentation, and molecular chaperone activity. Its enrichment therefore reflects the activation of shared cellular stress–related mechanisms rather than a virus-specific response. These pathways are known to play critical roles in the heat stress response, further supporting the notion that high-temperature exposure induces ER stress, activates immune-related pathways, and regulates molecular chaperone expression to maintain cellular homeostasis [42–44]. A similar time-dependent transcriptional trend has also been reported in *Ctenopharyngodon idellus*. In a transcriptomic study by Zhang et al., the liver and brain tissues of grass carp under heat stress showed significant early enrichment in protein processing in the ER and immune-related pathways, suggesting that thermal stress rapidly initiates mechanisms related to cellular homeostasis and immune regulation [45].

To gain a functional overview of heat stress–induced transcriptomic responses, we conducted KEGG enrichment analyses for DEGs uniquely induced by heat stress at 6 h and 24 h. At 6 h, the significantly enriched pathways were primarily related to protein folding and metabolism, including Protein processing in endoplasmic reticulum, Ascorbate and aldarate metabolism, Protein export, and Porphyrin and chlorophyll metabolism, suggesting that early heat stress triggers rapid activation of protein quality-control and metabolic adjustment mechanisms [46]. In contrast, at 24 h, the uniquely induced DEGs were enriched in a broader set of immune-related and pathogen-recognition pathways, such as Influenza A, NOD-like receptor signaling pathway, RIG-I-like receptor signaling pathway, Toll-like receptor signaling pathway, and Antigen processing and presentation, along with metabolic pathways including Glutathione metabolism and Arginine and proline metabolism [47,48]. This shift indicates that prolonged heat exposure promotes enhanced innate immune signaling and metabolic adaptation.

Comparative analysis of the shared DEGs between 6 h and 24 h revealed consistent activation of classical stress-responsive pathways under high-temperature exposure. Hierarchical clustering showed that several molecular chaperone genes—including *hspa5, hspa4l, hsp90b1*, and *dnajc3a*—were continuously upregulated at both time points. These genes play essential roles in the ER stress response and protein folding regulation. Under heat-induced damage or accumulation of misfolded proteins, their expression is rapidly induced to assist in the recognition and repair of denatured proteins, thereby maintaining ER homeostasis and overall intracellular stability [49,50]. In addition, genes such as syvn1, uggt1, sel1l, and pdia4/pdia6 were also significantly upregulated. These genes are critical components of the ER-associated degradation (ERAD) pathway and protein quality control system [51,52], indicating that yellowfin tuna rapidly activates proteostasis mechanisms under thermal stress to mitigate cellular damage. In contrast, genes including *KRAB*, *ifih1*, *MHC1*, and *srsf5b* were significantly downregulated during high-temperature exposure. Notably, the suppression of *MHC1* suggests that the capacity for antigen recognition and presentation may be impaired under sustained heat stress, reflecting a potential complexity in immune system regulation [53]. Meanwhile, *ifih1*, a pattern recognition receptor (PRR) involved in antiviral responses, exhibited decreased expression, possibly indicating disruption of innate immune signaling pathways under thermal conditions [54]. Interestingly, the gradual reduction of heat shock protein–related transcriptional signatures at 24 h, together with the decline in immune-associated gene activity, may indicate a physiological transition from acute stress defense toward early thermal acclimation. This pattern suggests that heat shock proteins could participate in a compensatory regulatory mechanism that helps restore cellular stability and metabolic balance once the initial stress response has been triggered [55]. These findings collectively demonstrate that under heat stress, the organism simultaneously activates ER protein processing and molecular chaperone pathways while exhibiting a potential suppression in certain immune recognition modules, highlighting a finely tuned and dynamic regulatory strategy across multiple pathways in response to thermal stress.

Furthermore, analysis of the constructed PPI network provided additional support for the central roles of several stress-responsive genes during heat exposure. This network comprised 27 genes, exhibiting a tightly connected structure and high interaction density, and was generated using high-confidence protein–protein interactions from the STRING database. Hub genes such as *pdia4*, *hspa5*, *dnajc3a*, *hspa4l*, *hsp90b1*, *calr3a*, *hyou1*, and *pdia6* displayed high connectivity degrees, a pattern consistent with their established functions in coordinating ER stress responses, protein folding, and proteostasis regulation during heat exposure [56]. Although these genes encode molecular chaperones rather than classical transcriptional regulators, their central positions within the network reflect their roles as integrators of unfolded protein response (UPR) and ER-associated degradation (ERAD) signaling [57].

Notably, intensive interactions were observed between members of the protein disulfide isomerase (PDI) family, such as *pdia4*, *pdia6*, and *pdia3*, and molecular chaperones including *hspa5* and *hsp90b1* [58], forming a functional module centered on ER protein folding regulation. This supports the notion that cells enhance protein processing capacity to mitigate the stress burden caused by the accumulation of misfolded proteins under heat stress [59]. Heat shock proteins such as *dnajc3a*, *hspa4l*, and hyou1 also exhibited notable centrality within the network, suggesting their rapid engagement in the molecular chaperone system during the early phases of stress response [60]. Although genes like *syvn1*, *uggt1*, and *sel1l* were located on the network periphery, they demonstrated clear interactions with central nodes and are primarily involved in the ERAD pathway. This suggests that under heat stress, the ERAD mechanism may be co-activated to facilitate the recognition and clearance of misfolded proteins [61]. In contrast, nodes such as *KRAB*, *SEC24*, and rheb showed low connectivity and were positioned at the network margin, implying that they may not be directly involved in the core heat-induced stress response. Similarly, although *MHC1*, *srsf5b*, and *ifih1* were significantly downregulated at the transcriptomic level, they did not exhibit high interaction features within the PPI network. This further indicates that under the current stress condition, the organism prioritizes activation of ER protein processing and folding systems to maintain homeostasis [62,63], while the immune recognition pathways may exhibit a relatively suppressed status.

5. Conclusions

This study investigated the hepatic transcriptomic responses of juvenile *Thunnus albacares* under high-temperature stress (34 °C) compared to a normal temperature control (28 °C) at 6 h and 24 h. The results showed a greater number of DEGs at 6 h, indicating a more intense early stress response. The shared DEGs were significantly enriched in pathways related to protein processing in the endoplasmic reticulum, immune regulation, and viral infection, suggesting that the organism responds to heat stress mainly through adjustments in protein homeostasis and cellular stress management rather than directional immune activation.

PPI analysis revealed that genes such as *pdia4*, *hspa5*, *dnajc3a*, and *hsp90b1* acted as central regulators involved in protein folding and endoplasmic reticulum homeostasis during heat stress. Their roles suggest that yellowfin tuna increase protein folding capacity to mitigate misfolded protein accumulation under thermal stress. In contrast, the reduced connectivity and lower expression of immune-associated genes such as *mhc1* and *ifih1* suggest a suppression or functional downscaling of immune signaling during the acute phase of heat stress, rather than an activation of immune pathways.

Supplementary Materials

The additional data and information can be downloaded at: https://media.sciltp.com/articles/others/2601071423324656/ALE-25090088-Supplementary_Materials.zip.

Author Contributions

J.H.: Methodology; Investigation; Validation; Data curation; Writing—review & editing. Z.F.: Formal analysis; Software; Visualization; Writing—original draft; Writing—review & editing. J.B.: Investigation; Validation; Resources. Z.M.: Conceptualization; Supervision; Project administration; Funding acquisition; Writing—review & editing. All authors have read and agreed to the published version of the manuscript.

Funding

This research was funded by the National Natural Science Foundation of China (32460927), Science and Technology special fund of Hainan Province (grant number ZDYF2024XDNY247), the Central Public-interest Scientific Institution Basal Research Fund, CAFS (2025XT03, 2023TD58) and the Project of the Department of Science, Technology and Education, Ministry of Agriculture and Rural Affairs of the People's Republic of China (019250367).

Institutional Review Board Statement

Animal handling and experimental procedures complied with the ethical standards of the Animal Care and Use Committee of the South China Sea Fisheries Research Institute (Chinese Academy of Fishery Sciences), with approval obtained before the study commenced.

Informed Consent Statement

Not applicable.

Data Availability Statement

All data generated or analyzed in this study are presented in the main text. The raw RNA-seq data are available from the corresponding author upon reasonable request.

Conflicts of Interest

The authors declare no conflict of interest.

Use of AI and AI-Assisted Technologies

During the preparation of this work, the authors used ChatGPT-5 to polish the English language. After using this tool, the authors reviewed and edited the content as needed and take full responsibility for the content of the published article.

References

1. Wernberg, T.; Thomsen, M.S.; Burrows, M.T.; et al. Marine Heatwaves as Hot Spots of Climate Change and Impacts on Biodiversity and Ecosystem Services. *Nat. Rev. Biodivers.* **2025**, *1*, 461–479. https://doi.org/10.1038/s44358-025-00058-5.
2. Moura, M.M.; Dos Santos, A.R.; Pezzopane, J.E.M.; et al. Relation of El Niño and La Niña Phenomena to Precipitation, Evapotranspiration and Temperature in the Amazon Basin. *Sci. Total Environ.* **2019**, *651*, 1639–1651. https://doi.org/10.1016/j.scitotenv.2018.09.242.
3. Thirumalai, K.; DiNezio, P.N.; Okumura, Y.; et al. Extreme Temperatures in Southeast Asia Caused by El Niño and Worsened by Global Warming. *Nat. Commun.* **2017**, *8*, 15531. https://doi.org/10.1038/ncomms15531.
4. Li, M.; Xu, Y.; Sun, M.; et al. Impacts of Strong ENSO Events on Fish Communities in an Overexploited Ecosystem in the South China Sea. *Biology* **2023**, *12*, 946. https://doi.org/10.3390/biology12070946.
5. Reynolds, W.W.; Casterlin, M.E. The Role of Temperature in the Environmental Physiology of Fishes. In *Environmental Physiology of Fishes*; Springer: Berlin/Heidelberg, Germany, 1980; pp. 497–518.
6. Chowdhury, S.; Saikia, S. Oxidative Stress in Fish: A review. *J. Sci. Res.* **2020**, *12*, 145–160. https://doi.org/10.3329/jsr.v12i1.41716.
7. Chen, Y.; Chen, S.-Q.; Zhang, B.; et al. Effects of Acute High-Temperature on Gill Tissue Structure, Serum Biochemical Indices, Antioxidant Capacity and Liver Transcriptomics of *Thamnaconus septentrionalis*. *J. Therm. Biol.* **2025**, *129*, 104098. https://doi.org/10.1016/j.jtherbio.2025.104098.
8. Bard, B.; Kieffer, J.D. The Effects of Repeat Acute Thermal Stress on the Critical Thermal Maximum (CTmax) and Physiology of Juvenile Shortnose Sturgeon (*Acipenser brevirostrum*). *Can. J. Zool.* **2019**, *97*, 567–572. https://doi.org/10.1139/cjz-2018-0157.
9. Munday, P.; Kingsford, M.; O'callaghan, M.; et al. Elevated Temperature Restricts Growth Potential of the Coral Reef Fish *Acanthochromis polyacanthus*. *Coral Reefs* **2008**, *27*, 927–931. https://doi.org/10.1007/s00338-008-0393-4.
10. Huang, J.; Fu, Z.; Bai, J.; et al. Cold Stress Disrupts Gill Homeostasis in Juvenile Yellowfin Tuna (*Thunnus albacares*) by Altering Oxidative, Metabolic, and Immune Responses. *Mar. Environ. Res.* **2025**, 107300. https://doi.org/10.1016/j.marenvres.2025.107300.
11. Franck, J.P.; Robinson, S.W. Endothermy in Fish: A Remarkable Story of Convergent Evolutionary Adaptation. In *Biochemistry of Non-Shivering Thermogenesis in Vertebrates*; CRC Press: Boca Raton, FL, USA, 2025; pp. 55–66.
12. Muñoz-Abril, L.J. Biology and Connectivity of Yellowfin Tuna in the Eastern Pacific Ocean. Doctoral Dissertation, University of South Alabama, Mobile, AL, USA, 2024.
13. Schaefer, K.M.; Fuller, D.W.; Block, B.A. Movements, Behavior, and Habitat Utilization of Yellowfin Tuna (*Thunnus albacares*) in the Northeastern Pacific Ocean, Ascertained through Archival Tag Data. *Mar. Biol.* **2007**, *152*, 503–525. https://doi.org/10.1007/s00227-007-0689-x.
14. Jayasundara, N.; Gardner, L.D.; Block, B.A. Effects of Temperature Acclimation on Pacific Bluefin Tuna (*Thunnus orientalis*) Cardiac Transcriptome. *Am. J. Physiol. Regul. Integr. Comp. Physiol.* **2013**, *305*, R1010–R1020. https://doi.org/10.1152/ajpregu.00254.2013.
15. Fu, Z.; Bai, J.; Ma, Z. Physiological Adaptations and Stress Responses of Juvenile Yellowfin Tuna (*Thunnus albacares*) in Aquaculture: An Integrative Review. *Aquat. Life Ecosyst.* **2025**, *1*, 3.
16. Liu, H.; Fu, Z.; Yu, G.; et al. Effects of Acute High-Temperature Stress on Physical Responses of Yellowfin Tuna (*Thunnus albacares*). *J. Mar. Sci. Eng.* **2022**, *10*, 1857. https://doi.org/10.3390/jmse10121857.
17. Liu, H.; Yang, R.; Fu, Z.; et al. Acute Thermal Stress Increased Enzyme Activity and Muscle Energy Distribution of Yellowfin Tuna. *PLoS ONE* **2023**, *18*, e0289606. https://doi.org/10.1371/journal.pone.0289606.
18. Mokhtar, D.M.; Zaccone, G.; Alesci, A.; et al. Main Components of Fish Immunity: An Overview of the Fish Immune

System. *Fishes* **2023**, *8*, 93. https://doi.org/10.3390/fishes8020093.
19. Wang, M.; Xu, G.; Tang, Y.; et al. Investigation of the Molecular Mechanisms of Antioxidant Damage and Immune Response Downregulation in Liver of *Coilia nasus* Under Starvation Stress. *Front. Endocrinol.* **2021**, *12*, 622315. https://doi.org/10.3389/fendo.2021.622315.
20. Jia, R.; Du, J.; Cao, L.; et al. Antioxidative, Inflammatory and Immune Responses in Hydrogen Peroxide-Induced Liver Injury of Tilapia (GIFT, *Oreochromis niloticus*). *Fish Shellfish. Immunol.* **2019**, *84*, 894–905. https://doi.org/10.1016/j.fsi.2018.10.084.
21. Liu, E.; Zhao, X.; Li, C.; et al. Effects of Acute Heat Stress on Liver Damage, Apoptosis and Inflammation of Pikeperch (*Sander lucioperca*). *J. Therm. Biol.* **2022**, *106*, 103251. https://doi.org/10.1016/j.jtherbio.2022.103251.
22. Roychowdhury, P.; Aftabuddin, M.; Pati, M.K. Thermal Stress-Induced Oxidative Damages in the Liver and Associated Death in Fish, *Labeo rohita*. *Fish Physiol. Biochem.* **2021**, *47*, 21–32. https://doi.org/10.1007/s10695-020-00880-y.
23. Feidantsis, K.; Georgoulis, I.; Zachariou, A.; et al. Energetic, Antioxidant, Inflammatory and Cell Death Responses in the Red Muscle of Thermally Stressed *Sparus aurata*. *J. Comp. Physiol. B* **2020**, *190*, 403–418. https://doi.org/10.1007/s00360-020-01278-1.
24. Sudhagar, A.; Kumar, G.; El-Matbouli, M. Transcriptome Analysis Based on RNA-Seq in Understanding Pathogenic Mechanisms of Diseases and the Immune System of Fish: A Comprehensive Review. *Int. J. Mol. Sci.* **2018**, *19*, 245. https://doi.org/10.3390/ijms19010245.
25. Liu, Y.; Tian, C.; Yang, Z.; et al. Effects of Chronic Heat Stress on Growth, Apoptosis, Antioxidant Enzymes, Transcriptomic Profiles, and Immune-Related Genes of Hong Kong Catfish (*Clarias fuscus*). *Animals* **2024**, *14*, 1006. https://doi.org/10.3390/ani1407100.
26. Long, Y.; Li, L.; Li, Q.; et al. Transcriptomic Characterization of Temperature Stress Responses in Larval Zebrafish. *PLoS ONE* **2012**, *7*, e37209. https://doi.org/10.1371/journal.pone.0037209.
27. Beemelmanns, A.; Zanuzzo, F.S.; Xue, X.; et al. The Transcriptomic Responses of *Atlantic salmon* (*Salmo salar*) to High Temperature Stress Alone, and in Combination with Moderate Hypoxia. *BMC Genom.* **2021**, *22*, 261. https://doi.org/10.1186/s12864-021-07464-x.
28. Zhao, T.; Ma, A.; Yang, S.; et al. Integrated Metabolome and Transcriptome Analyses Revealing the Effects of Thermal Stress on Lipid Metabolism in Juvenile Turbot *Scophthalmus maximus*. *J. Therm. Biol.* **2021**, *99*, 102937. https://doi.org/10.1016/j.jtherbio.2021.102937.
29. Deng, K.; Yang, S.; Gu, D.; et al. Record-Breaking Heat Wave in Southern China and Delayed Onset of South China Sea Summer Monsoon Driven by the Pacific Subtropical High. *Clim. Dyn.* **2020**, *54*, 3751–3764. https://doi.org/10.1007/s00382-020-05203-8.
30. Li, Y.; Ren, G.; Wang, Q.; et al. Changes in Marine Hot and Cold Extremes in the China Seas During 1982–2020. *Weather Clim. Extrem.* **2023**, *39*, 100553.
31. Huang, J.; Fu, Z.; Liu, X.; et al. Splenic Tissue Injury and Physiological Response Mechanisms in Juvenile Yellowfin Tuna (*Thunnus albacares*) Under Acute Cold Stress. *Dev. Comp. Immunol.* **2025**, 105421. https://doi.org/10.1016/j.dci.2025.105421.
32. Amaral Carneiro, G.; Calì, M.; Cappelletti, E.; et al. Draft Genome Sequence of the Apple Pathogen *Colletotrichum chrysophilum* Strain M932. *J. Plant Pathol.* **2023**, *105*, 1141–1143. https://doi.org/10.1007/s42161-023-01353-w.
33. Kim, D.; Paggi, J.M.; Park, C.; et al. Graph-Based Genome Alignment and Genotyping with HISAT2 and HISAT-Genotype. *Nat. Biotechnol.* **2019**, *37*, 907–915. https://doi.org/10.1038/s41587-019-0201-4.
34. Xu, C.; Song, L.Y.; Li, J.; et al. MangroveDB: A Comprehensive Online Database for Mangroves Based on Multi-Omics Data. *Plant Cell Environ.* **2025**, *48*, 2950–2962. https://doi.org/10.1111/pce.15318.
35. Lucchesi, S.; Montesi, G.; Polvere, J.; et al. Transcriptomic Analysis After SARS-CoV-2 mRNA Vaccination Reveals a Specific Gene Signature in Low-Responder Hemodialysis Patients. *Front. Immunol.* **2025**, *16*, 1508659.
36. Varet, H.; Brillet-Guéguen, L.; Coppée, J.-Y.; et al. SARTools: A DESeq2-and EdgeR-Based R Pipeline for Comprehensive Differential Analysis of RNA-Seq Data. *PLoS ONE* **2016**, *11*, e0157022. https://doi.org/10.1371/journal.pone.0157022.
37. Lancelle, L.J.; Potru, P.S.; Spittau, B.; et al. DgeaHeatmap: An R Package for Transcriptomic Analysis and Heatmap Generation. *Bioinform. Adv.* **2025**, *5*, vbaf194. https://doi.org/10.1093/bioadv/vbaf194.
38. Nathaniel, T.P.; Chatterjee, N.S.; Varghese, T.; et al. Untargeted Metabolomics Reveals Membrane Lipid Remodeling and Dysregulation of Energy Metabolism in Genetically Improved Farmed Tilapia (*Oreochromis niloticus*) Under Acute Thermal Stress. *Aquaculture* **2025**, 743094. https://doi.org/10.1016/j.aquaculture.2025.743094.
39. Yang, X.; Wang, L.; Lu, K.; et al. High Temperature Changes the Structure and Function of Spotted Seabass (*Lateolabrax maculatus*) Tissues and Causes ER Stress and Mitochondrial Homeostasis Imbalance in Liver. *Aquaculture* **2025**, *599*, 742107.
40. Sarapultsev, A.; Komelkova, M.; Lookin, O.; et al. Zebrafish as a Model Organism for Post-Traumatic Stress Disorder: Insights into Stress Mechanisms and Behavioral Assays. *Biology* **2025**, *14*, 939. https://doi.org/10.3390/biology14080939.

41. Ahi, E.P.; Lindeza, A.S.; Miettinen, A.; et al. Transcriptional Responses to Changing Environments: Insights from Salmonids. *Rev. Fish Biol. Fish.* **2025**. https://doi.org/10.1007/s11160-025-09928-9.
42. Shi, X.; Cheng, Z.; Zheng, C.; et al. The Blood Transcriptome of Musk Deer Under Heat Stress Condition Reveals the Regulatory Mechanism of Genes to Maintain Homeostasis Metabolism. *BMC Genom.* **2025**, *26*, 400. https://doi.org/10.1186/s12864-025-11577-y.
43. Dilawari, R.; Chaubey, G.K.; Priyadarshi, N.; et al. Antimicrobial Peptides: Structure, Function, Mechanism of Action and Therapeutic Applications in Human Diseases. *Explor. Drug Sci.* **2025**, *3*, 1008110. https://doi.org/10.37349/eds.2025.1008110.
44. Chang, Q.; Zhang, Y.; Liu, X.; et al. Oxidative Stress in Antigen Processing and Presentation. *MedComm. Oncol.* **2025**, *4*, e70020. https://doi.org/10.1002/mog2.70020.
45. Zhang, W.; Xu, X.; Li, J.; et al. Transcriptomic Analysis of the Liver and Brain in Grass Carp (*Ctenopharyngodon idella*) Under Heat Stress. *Mar. Biotechnol.* **2022**, *24*, 856–870. https://doi.org/10.1007/s10126-022-10148-6.
46. Cecarini, V.; Gee, J.; Fioretti, E.; et al. Protein Oxidation and Cellular Homeostasis: Emphasis on Metabolism. *Biochim. Et Biophys. Acta (BBA)-Mol. Cell Res.* **2007**, *1773*, 93–104. https://doi.org/10.1016/j.bbamcr.2006.08.039.
47. Malik, G.; Zhou, Y. Innate Immune Sensing of Influenza A Virus. *Viruses* **2020**, *12*, 755. https://doi.org/10.3390/v12070755.
48. Le, J.; Kulatheepan, Y.; Jeyaseelan, S. Role of Toll-Like Receptors and Nod-Like Receptors in Acute Lung Infection. *Front. Immunol.* **2023**, *14*, 1249098. https://doi.org/10.3389/fimmu.2023.1249098.
49. Tian, Y.; Li, L.; Long, H.; et al. Transcriptome Analyses Reveal the Molecular Response of Juvenile Greater Amberjack (*Seriola dumerili*) to Marine Heatwaves. *Animals* **2025**, *15*, 1871. https://doi.org/10.3390/ani15131871.
50. Goutami, L.; Jena, S.R.; Moharana, A.K.; et al. HSPA2 Emerges as a Key Biomarker: Insights from Global Lysine Acetylproteomic Profiling in Idiopathic Male Infertility. *Cell Stress Chaperones* **2025**, *30*, 100090.
51. Gariballa, N.; Ali, B.R. Endoplasmic Reticulum Associated Protein Degradation (ERAD) in the Pathology of Diseases Related to TGFβ Signaling Pathway: Future Therapeutic Perspectives. *Front. Mol. Biosci.* **2020**, *7*, 575608. https://doi.org/10.3389/fmolb.2020.575608.
52. Pierre, A.S.; Gavriel, N.; Guilbard, M.; et al. Modulation of Protein Disulfide Isomerase Functions by Localization: The Example of the Anterior Gradient Family. *Antioxid. Redox Signal.* **2024**, *41*, 675–692. https://doi.org/10.1089/ars.2024.0561.
53. Taylor, B.C.; Balko, J.M. Mechanisms of MHC-I Downregulation and Role in Immunotherapy Response. *Front. Immunol.* **2022**, *13*, 844866. https://doi.org/10.3389/fimmu.2022.844866.
54. Thompson, M.R.; Kaminski, J.J.; Kurt-Jones, E.A.; et al. Pattern Recognition Receptors and the Innate Immune Response to Viral Infection. *Viruses* **2011**, *3*, 920.
55. Brasseur, M.V.; Bakowski, C.; Christie, M.; et al. Heat Stress Responsive Genes Are Not Affected by Ocean Warming: Long-Term Environmental Monitoring and Acute Thermal Stress Experiments Identify Non-Overlapping Sets of Differentially Expressed Genes in a Marine Fish. *Res. Sq.* **2025**. https://doi.org/10.21203/rs.3.rs-7212941/v1.
56. Díaz-Villanueva, J.F.; Díaz-Molina, R.; García-González, V. Protein Folding and Mechanisms of Proteostasis. *Int. J. Mol. Sci.* **2015**, *16*, 17193–17230.
57. Currie, J.; Manda, V.; Robinson, S.K.; et al. Simultaneous Proteome Localization and Turnover Analysis Reveals Spatiotemporal Features of Protein Homeostasis Disruptions. *Nat. Commun.* **2024**, *15*, 2207. https://doi.org/10.1038/s41467-024-46600-5.
58. Rahman, N.S.A.; Zahari, S.; Syafruddin, S.E.; et al. Functions and Mechanisms of Protein Disulfide Isomerase Family in Cancer Emergence. *Cell Biosci.* **2022**, *12*, 129. https://doi.org/10.1186/s13578-022-00868-6.
59. Schröder, M. Endoplasmic Reticulum Stress Responses. *Cell. Mol. Life Sci.* **2008**, *65*, 862–894. https://doi.org/10.1007/s00018-007-7383-5.
60. Singh, M.K.; Shin, Y.; Ju, S.; et al. Heat Shock Response and Heat Shock Proteins: Current Understanding and Future Opportunities in Human Diseases. *Int. J. Mol. Sci.* **2024**, *25*, 4209. https://doi.org/10.3390/ijms25084209.
61. Gao, C.; Peng, X.; Zhang, L.; et al. Proteome and Ubiquitylome Analyses of Maize Endoplasmic Reticulum under Heat Stress. *Genes* **2023**, *14*, 749. https://doi.org/10.3390/genes14030749.
62. Xu, C.; Evensen, Ø.; Munang'andu, H.M. Transcriptome Analysis Shows that IFN-I Treatment and Concurrent SAV3 Infection Enriches MHC-I Antigen Processing and Presentation Pathways in Atlantic Salmon-Derived Macrophage/Dendritic Cells. *Viruses* **2019**, *11*, 464. https://doi.org/10.3390/v11050464.
63. Esmaeili, N.; Martyniuk, C.J.; Kadri, S.; et al. Endoplasmic Reticulum Stress in Aquaculture Species. *Rev. Aquac.* **2025**, *17*, e70036. https://doi.org/10.1111/raq.70036.